Springer

KSME

Journal of Mechanical Science and Technology 33 (2) (2019) 837~845
www.springerlink.com/content/1738-494x(Print)/1976-3824(Online)
DOI 10.1007/s12206-019-0140-5

Skidding analysis of angular contact ball bearing subjected to radial load and angular misalignment †

Laily Oktaviana[1], Van-Canh Tong[2] and Seong-Wook Hong[1,*]

[1]*Department of Mechanical System Engineering, Kumoh National Institute of Technology, 61 Daehak-ro, Gumi, Gyeongbuk 39177, Korea*
[2]*Department of Ultra-Precision Machines and Systems, Korea Institute of Machinery and Materials, 156 Gajeongbuk-ro, Daejeon 34103, Korea*

(Manuscript Received July 27, 2018; Revised October 13, 2018; Accepted October 16, 2018)

Abstract

Skidding is a phenomenon that frequently occurs in ball–raceway contact areas of bearings and often leads to their early failure. This paper presents a skidding analysis of angular contact ball bearings (ACBBs) subjected to various boundary conditions. A five degrees-of-freedom quasi-static model for ACBBs was employed to investigate skidding with ball and race contact forces and inertial loading by rotational speed. The model provided the internal load distribution of all rolling elements, which was subsequently used for the skidding prediction. Hirano's criterion was used as a theoretical basis for the skidding analysis of ACBBs. Simulations were performed to investigate the influence of external loading, rotational speed, and angular misalignment on the bearing skidding. The effects of the preload method and initial contact angle on the skidding were also considered. As a result, this study provided an in-depth observation of skidding in ACBBs subjected to various operating conditions.

Keywords: Angular contact ball bearing; Angular misalignment; Preload; Radial load; Skidding

1. Introduction

Rolling element bearings are essential in rotating machines. Among others, angular contact ball bearings (ACBBs) have been extensively used in practice for main spindles of machine tool systems, gas turbines, engines, electric generators, etc. [1-4]. The major advantages of ACBBs are the ability to withstand combined axial and radial loads, as well as the capability to operate under high rotational speed with excellent accuracy. Research on the static and dynamic characteristics of ACBBs has received significant attention by worldwide researchers and, consequently, great advances have been attained and contributed to the design and manufacture of ACBBs.

Skidding is a phenomenon that frequently occurs on ball–raceway contact areas caused by insufficient traction at the contact. The skidding in an ACBB may cause unstable cage speed, increasing operating temperature, and premature failure of the bearing. Therefore, researchers have made significant efforts to investigate the skidding problem in order to aid engineers in the practical design and application of ACBBs [5-10].

The theoretical analysis of skidding in rolling bearings can be broadly categorized into two groups. The first group attempted to discover preferable applied loads, beyond which the skidding phenomenon in ACBBs can be avoided. The researchers commonly developed empirical formulae, which identify the required preload to avoid skidding, e.g., the works of Hirano and Tanoue [5, 6]. Boness [7] also proposed an empirical equation for the required maximum Hertzian pressure at the ball and inner race contact. The proposed formula includes the effect of lubricant viscosity at the operating temperature. Liao and Lin [8] adopted the formula proposed by Hirano to investigate the skidding of ACBBs considering axial and radial deformations of the inner ring. Xu et al. [9] also used Hirano's approach to determine the proper axial preload for different speed ranges to avoid skidding in ACBBs.

The second group analyzed the motion of bearing components, from which the occurrence of skidding can be detected. In this way, the cage speed was often calculated and compared with its theoretical value to identify whether or not skidding occurred. Accordingly, a quite straightforward approach is to characterize the skidding based on an analytical quasi-static bearing model [10-14]. Harris [10] outlined an analytical method to predict skidding in high-speed roller bearings. Later, he extended this approach to predict the skidding of thrust-loaded ACBBs [11]. Boness and Gentle [12, 13] also used the quasi-static approach to formulate a set of eight equilibrium equations for the balls and races of thrust-loaded ball bearings.

*Corresponding author. Tel.: +82 54 478 7344, Fax.: +82 54 478 7319
E-mail address: swhong@kumoh.ac.kr
† Recommended by Associate Editor Young Hun Jeong

Then, the equations can be solved to determine the ball orbital or the cage speed. In addition to the quasi-static model, researchers also developed full dynamic equations of bearings, which have recently attracted significant attention [15-20]. A number of bearing dynamic models with varying the degree of complexity have been proposed. One of the most significant advantages of this approach is the capability of providing adequate information of the ball and race dynamical characteristics.

From the above literature review, it is observed that most studies considered thrust-loaded bearings. The effect of combined loading on the skidding of a bearing has rarely been addressed. In addition, to the authors' best knowledge, the skidding behavior in the presence of angular misalignment has not yet been considered. It is also evident that the effect of the preload method on the skidding of ball bearings has not been discussed. To address the aforementioned issues, we investigate the skidding of ACBBs in consideration of the effects of various boundary conditions. This paper is structured as follows: In Sec. 2, we present a quasi-static bearing model, which provides the internal contact load distribution, contact angles of the ball and races, and inertial load of the balls. Then, the Hirano's method based on a quasi-static model for analyzing the skidding of ACBBs is outlined. We also compare the numerical results of minimum preload to prevent skidding predicted by Hirano's criterion and experimental data from the literature, which validates the proposed method used in further skidding analysis. Sec. 3 presents numerical simulations that were performed to further investigate the skidding behavior of a sample ACBB. We consider the effect of various operating conditions on the skidding such as combined loading, rotational speed, and angular misalignment. We also investigate the effect of certain important factors on the bearing skidding such as the unloaded contact angle and preload method. Finally, in Sec. 4, the conclusions of this study are drawn.

2. Determination of skidding in ACBB

2.1 Quasi-static model of ACBB

The ball bearing model proposed by de Mul et al. [21] is adopted in this study. Fig. 1 shows a five degrees-of-freedom (DOFs) model of an ACBB with the global coordinates system, loading and displacement. The load vector $\{F\}^{\mathrm{T}} = \{F_x, F_y, F_z, M_x, M_y\}$ represents the external load applied to the inner ring, and the corresponding displacement vector is $\{\delta\}^{\mathrm{T}} = \{\delta_x, \delta_y, \delta_z, \gamma_x, \gamma_y\}$.

Fig. 2 describes the overall calculation process of the bearing model. The nonlinear equilibrium equations of the bearing can be iteratively solved to obtain the internal contact load of bearing. This iterative solution requires a global iteration loop for the equilibrium of inner ring, and the inner iteration loop for the equilibrium of each ball. Detailed description of inner ring and ball equilibrium equations are given in Appendix.

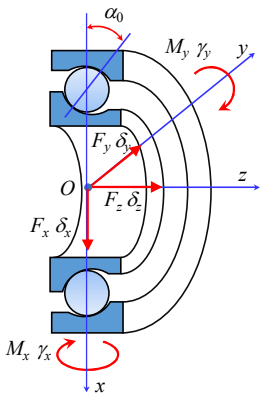

Fig. 1. Global coordinate system, loading and displacement.

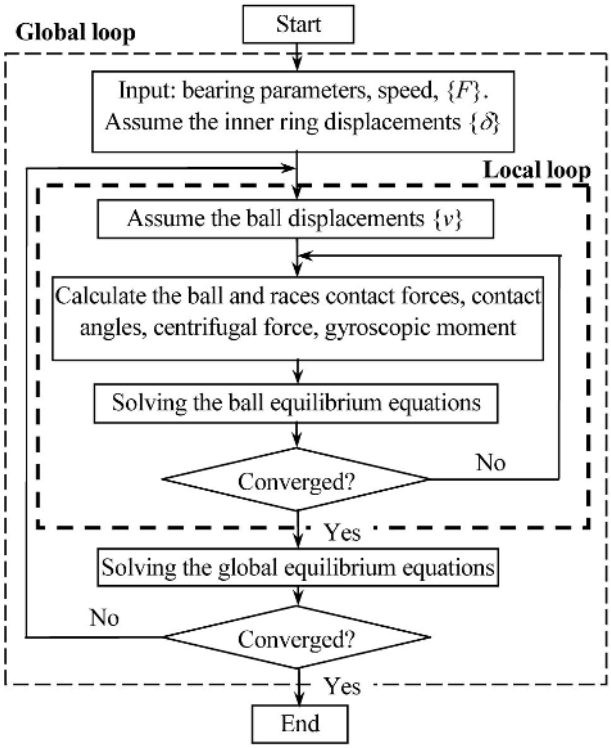

Fig. 2. Calculation process for ball bearing equilibrium.

2.2 ACBB skidding prediction

Skidding, which is defined by the gross sliding of the ball relative to the raceways in the rolling direction, can cause significant adverse effects on the performance of the bearing, such as wear of bearing elements or excessive heat generation [1, 10, 11]. There have been several analytical formulae for predicting skidding in ACBBs. Hirano [6] proposed an empirical skidding criterion applicable to ACBBs under thrust load (referred to as *Hirano's criterion*). The ball skidding can be avoided if the following condition is satisfied

$$\frac{Q_a}{F_c} > 10 \tag{1}$$

Table 1. Parameters of the simulated ACBB.

Young's modulus (GPa)	210
Bore diameter d	35
Outer diameter D	62
Pitch diameter d_m (mm)	48.51
Ball diameter D_a (mm)	6.5
Number of balls Z (mm)	15
Inner race curvature ratio κ_i	0.57
Outer race curvature ratio κ_o	0.54
Unloaded contact angle α_0 (deg)	15

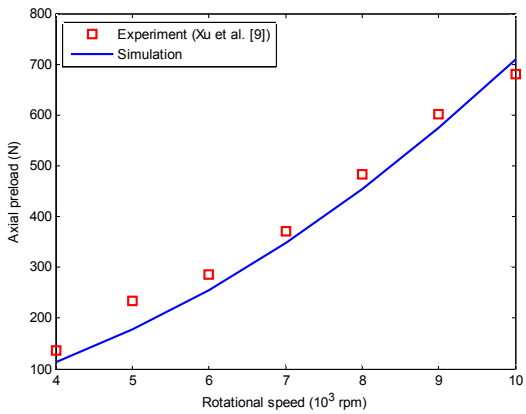

Fig. 3. Minimum preloads to avoid skidding as a function of rotational speed predicted by simulation and experiment [9].

where F_c is the centrifugal force acting on the ball, as given in Eq. (A.7) in Appendix. Q_a is the axial component of the ball–inner-race normal force Q_i, determined by

$$Q_a = Q_i \sin\alpha_i \,. \tag{2}$$

Substituting Eq. (2) into Eq. (1), one can obtain

$$SF = \frac{Q_i \sin\alpha_i}{F_c} > 10 \,. \tag{3}$$

Here, SF represents a "*skidding factor*", which determines the occurrence of skidding. The ball-to-inner-race contact force and contact angle are determined by using the ACBB model presented in the previous section.

Fig. 3 presents the minimum axial preload to avoid skidding as a function of rotational speed determined by Hirano's criterion [6]. The theoretical results are calculated for an ACBB B7007C with parameters shown in Table 1. Fig. 3 shows that the minimum axial preloads of an ACBB 7007C predicted by the theoretical model match well with experimental data. To further assess the skidding in ACBBs subjected to different boundary conditions, we perform simulations for a sample ACBB 7007C. The skidding behavior of the bearing is simulated by MATLAB.

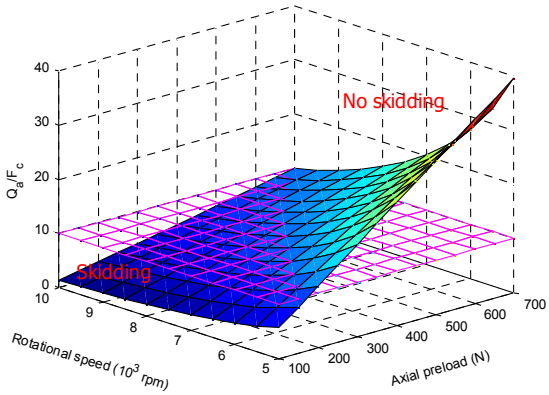

Fig. 4. Skidding factor of ACBB as a function of axial load and rotational speed.

3. Investigation of the skidding in ACBB

In this section, we present the numerical results of the analysis of skidding in an ACBB. The effects of various operating conditions on the skidding behavior are investigated. To determine whether the skidding of a ball occurs or not, the skidding factor, defined as Q_a/F_c, is calculated according to Hirano's criterion, which was described in Eq. (3).

To investigate the effects of the rotational speed and axial preload on the skidding of an ACBB, the bearing speed and axial preload are varied from 5000 rpm to 10000 rpm and 100 N to 700 N, respectively. For the case in which the bearing is axially loaded, all the balls experience identical contact load conditions. Therefore, the skidding factor of a representative ball can be calculated to examine the bearing skidding. The calculated results of the skidding factor are plotted in Fig. 4, which clearly shows two skidding and no-skidding regions distinguished by a horizontal plane at the threshold value of 10.0. The results in Fig. 4 show that an ACBB running at a higher rotational speed requires a larger axial preload to prevent the balls from skidding. At a preload below 100 N, skidding occurs over the entire speed range, whereas the skidding can be completely avoided with a preload of 700 N. Moreover, the skidding factor manifests a nonlinear variation with respect to applied load and rotational speed.

3.1 Effects of axial preload and rotational speed

According to Eq. (3), there are several internal dynamic quantities that directly affect the bearing skidding, i.e., the contact force, contact angle, and centrifugal force. These three factors are demonstrated in Figs. 5 and 6. It is observed that increasing the axial load leads to increases in the contact force and contact angles. As a result, decreasing the skidding possibility can be achieved by increasing the bearing preload. However, the centrifugal force increases with the rotational speed as illustrated in Fig. 6(a), which increases the skidding possibility of the bearing. In addition, with the increase in centrifugal force, the contact force of the ball and outer race-

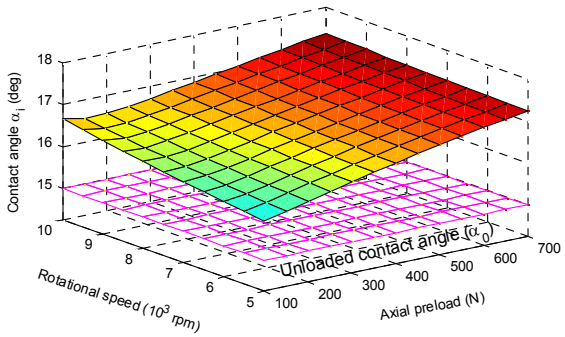

Fig. 5. Influence of axial preload and rotational speed on contact angle.

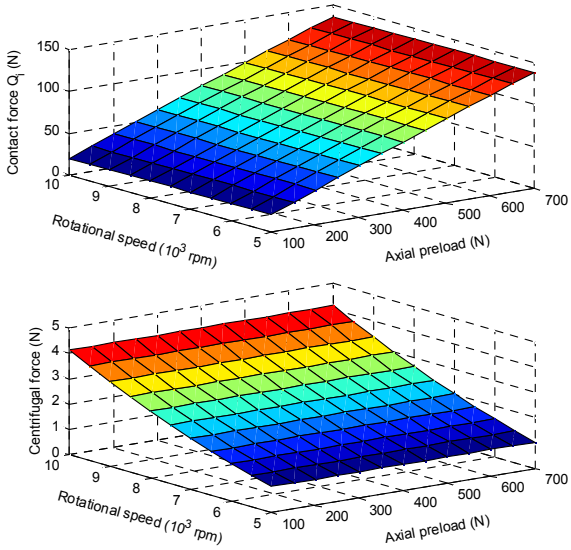

(a) Effect of axial preload and rotational speed on ball loading

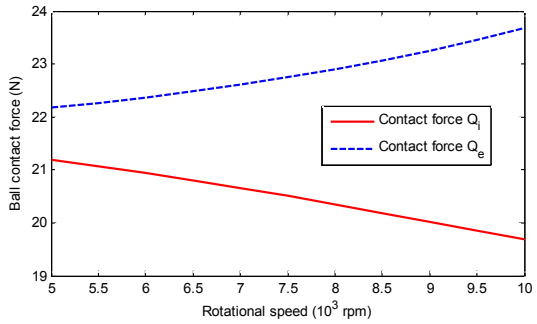

(b) Ball contact forces at preload 100 N

Fig. 6. Ball contact force and centrifugal force.

way would be increased because of the outward centrifugal force, as shown in Fig. 6(b). At the same time, the contact force of the ball and inner raceway is reduced, which also contributes to the increase in the skidding of the bearing at high speed.

3.2 Effect of combined radial and axial loads

In the case of an ACBB subjected to radial load, the contact

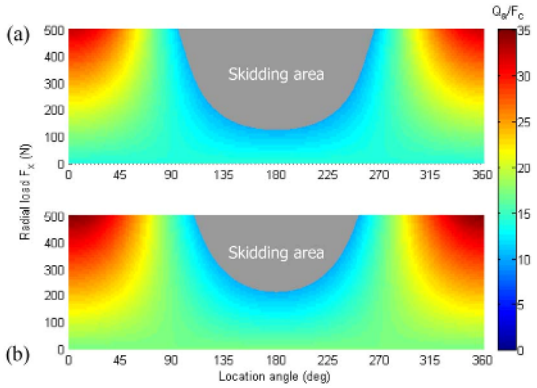

Fig. 7. Skidding regions under radial load (n = 5000 rpm): (a) F_z = 250 N; (b) F_z = 300 N.

load between the ball and raceway varies depending on its circumferential angle on the raceway. Therefore, the skidding factor of the individual ball should be simulated. To investigate the skidding behavior of a radially loaded ACBB, the radial load is selected from 0 N to 500 N. The bearing is assumed to be properly aligned and preloaded by constant preload of 250 N and 300 N. Fig. 7 displays the effect of radial load on the skidding behavior of an ACBB operating at the rotational speed of 5000 rpm. It is observed that when the applied radial load exceeds a certain limit value, there occurs a skidding area around circumferential angle 180°, i.e., the top of the bearing indicated by a shaded-grey area. Increasing the radial load leads to an enlargement of the skidding area, which is caused by the decrease in the ball–raceway contact forces at the corresponding location under radial load. Higher axial preload can narrow down the skidding area; for example, the skidding starts occurring at a radial load of 110 N for a 250 N preload [Fig. 7(a)], whereas the skidding occurs at approximately 200 N for a 300-N preload [Fig. 7(b)].

To investigate the skidding behavior of an individual ball in an ACBB under combined radial and axial loads, Figs. 8(a) and (b) show the critical lines of the balls determined at the rotational speeds of 5000 and 6000 rpm, respectively. A point on the critical line defines the applied radial and axial loads at which the skidding factor of the ball reaches the critical value of 10.0, as shown in Eq. (3). Consequently, a point located on the right side of the critical line of a ball will define the applied loads under which skidding can be avoided for the designated ball. Owing to the inherent symmetry of the bearing about the vertical axis, only the critical lines for the balls on the half of the bearing are plotted, i.e., balls #1 to #9. It is seen that all the lines converge to a point at zero radial load, because under no radial load, i.e., pure axial loading, all the balls have identical loading conditions.

Fig. 8 further shows that with increasing radial load, the required axial loads for avoiding skidding of the balls at the bottom of the bearing, such as ball #1, 2 and 3 tend to reduce. On the contrary, the required axial loads of the balls at the top of bearing, such as ball #7, 8 and 9 tend to increase. These

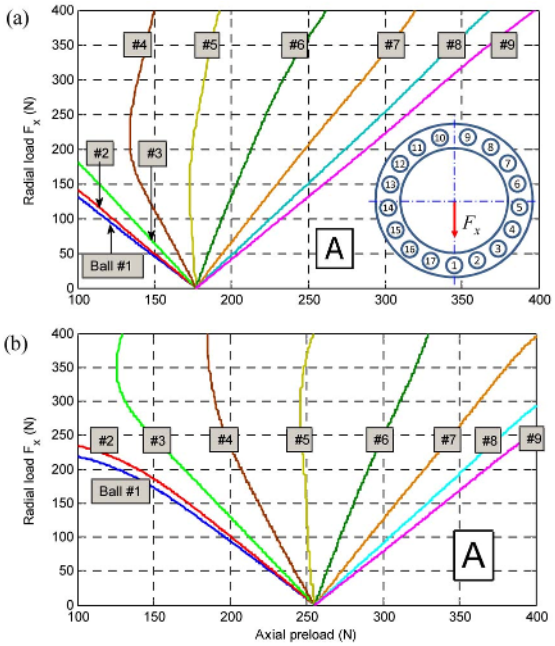

Fig. 8. Critical skidding lines of each ball in ACBB: (a) n = 5000 rpm; (b) n = 6000 rpm.

results agree with the skidding area presented in Fig. 7. In order to avoid skidding for all the balls, applied loads inside the region indicated by "A" in Figs. 8(a) and (b) should be selected. Moreover, the critical lines are shifted to the right with increasing rotational speed, which implies the reduction in the skidding-free area, as illustrated in Fig. 8(b).

3.3 Effect of angular misalignment

Misalignment is a common problem in rolling bearing applications. The initial mounting error is one of the frequent causes of bearing misalignment. In fact, although a bearing might be properly mounted, misalignment can still occur during operation owing to elastic bending in the shaft under loading. This consequently affects the mechanical performance of the bearing, such as fatigue life, stiffness, and mechanical wear. The harmful effect of misalignment on skidding of rolling bearings, however, has rarely been addressed.

3.3.1 Axially loaded bearing

Fig. 9 demonstrates the effect of angular misalignment varying from 0 to 3 mrad on the skidding of an ACBB. The bearing is preloaded by constant axial preloads of 250 N and 300 N, and the rotational speed is selected as 5000 rpm. It is clear that increasing misalignment angle results in increased skidding in the bearing. This is because the occurrence of misalignment redistributes the ball contact forces; the problem has been extensively discussed earlier by the authors [22-24]. Fig. 9 also depicts that with the angular misalignment below 1.0 mrad, the skidding problem can be avoided under the medium preload and rotational speed. This means that a permissible misalignment value of 1.0 mrad, which is provided by bearing manufactures for the bearing B7007C, [25, 26], can be used to avoid skidding under average condition. It should be also noted that increasing preload can reduce the skidding area, as shown in Fig. 9.

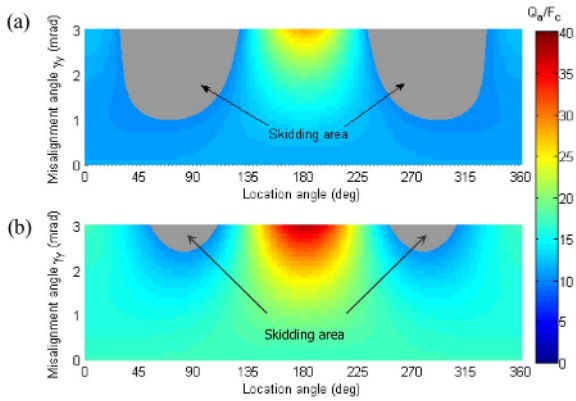

Fig. 9. Effect of angular misalignment on the skidding of ACBB load (n = 5000 rpm): (a) F_z = 250 N; (b) F_z = 300 N.

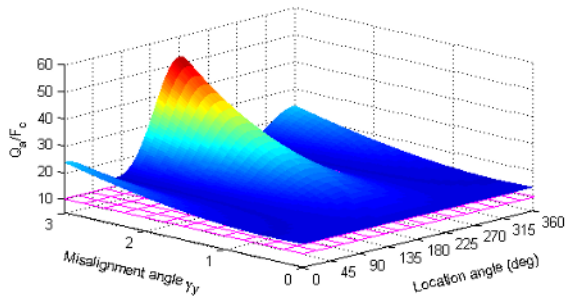

Fig. 10. Effect of angular misalignment on the skidding of ACBB with constant-displacement preload (δ_z = 15.55 μm, n = 5000 rpm).

The preload method can have a significant effect on the load distribution of a bearing and thus the skidding behavior, especially in the case of misaligned bearings. Apart from the constant-force preload, another preload method commonly adopted in practice is the rigid or constant-displacement preload method, which creates a certain amount of relative displacement between the inner and outer race of the bearing by using an inserted shim or locknut. For the purpose of comparison with the constant-force preload, the displacement preload is set at 15.55 μm, which produces the same amount of 250 N preload in the aligned condition.

Fig. 10 shows the effect of angular misalignment on the skidding of an ACBB preloaded by the rigid preload method. It is interesting that the rigid preload method can provide skidding avoidance even at large misalignment angle. This is because the rigid preload generates induced axial load and moment load, as shown in Fig. 11.

3.3.2 Radially loaded bearing

Fig. 12 shows the effect of radial loading and misalignment angle on the skidding behavior of an ACBB operating at the

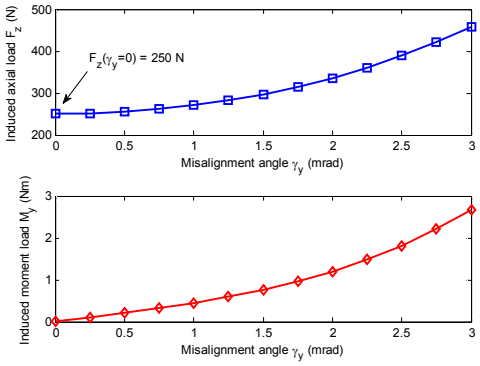

Fig. 11. Effect of misalignment angle on induced loads of ACBB with constant-displacement preload (δ_z = 15.55 μm and n = 5000 rpm).

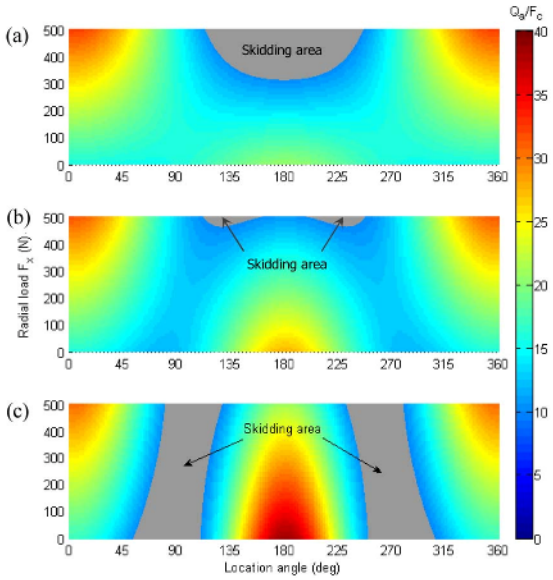

Fig. 12. Skidding under radial load (n = 5000 rpm): (a) γ_y = 1 mrad; (b) γ_y = 2 mrad; (c) γ_y = 3 mrad.

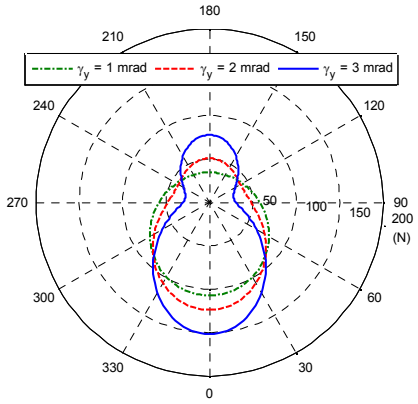

Fig. 13. Contact force between ball and inner race under different misalignment angles (n = 5000 rpm, F_x = 300 N, F_z = 300 N).

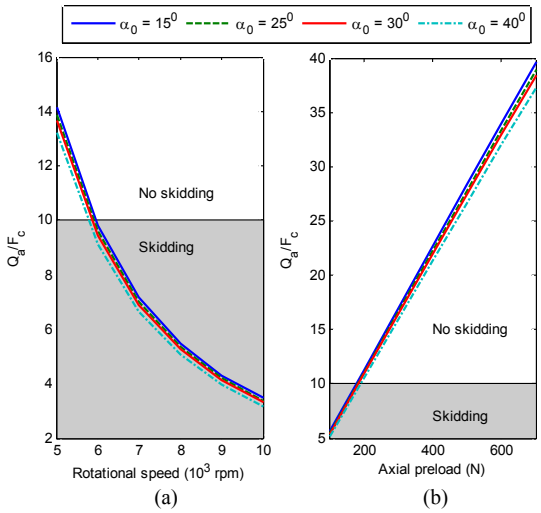

Fig. 14. Effect of unloaded contact angle on the skidding of ACBB without a radial load: (a) F_z = 250 N; (b) n = 5000 rpm.

rotational speed of 5000 rpm and the constant axial preload of 300 N. At low misalignment, there exists a skidding region around the circumferential angle of 180°. The increase in misalignment angle leads to the formation of two skidding regions around the circumferential angles of 90° and 270°. Because the rotational speed is kept constant at 5000 rpm, the ball contact force and contact angle are the two major factors causing the skidding condition to vary. Fig. 13 shows the contact force between the ball and inner race. The contact forces around the angles of 90° and 270° are found to reduce with increasing radial load. This indicates the formation of two corresponding skidding areas, as demonstrated in Fig. 12.

3.4 Effect of unloaded contact angle

The unloaded (or initial) contact angle is one of the important parameters that affect the load-carrying capacity of ACBBs [1, 27]. To be adopted for a wider range of application in practice, even the same ACBB series can be designed with different unloaded contact angles. The generally used values of unloaded contact angles for ACBBs are 15°, 25°, 30° and 40° [25]. The effect of the unloaded contact angle on the skidding of the ACBB is simulated and the results are shown in Figs. 14 and 15. Fig. 14 shows the simulated results for the skidding in the bearing under pure axial load. It is interesting that the unloaded contact angle has a minor influence on skidding for the entire range of rotational speed and axial preload without radial loading. However, the effect of the unloaded contact angle on the bearing skidding is remarkable in the case of radial loading, as shown in Fig. 15. It is observed that a higher unloaded contact angle would expand the skidding area. Therefore, a small unloaded contact angle could be suitable for preventing the skidding of the ACBB under radial loading.

4. Conclusions

In this paper, we have presented an analytical method for

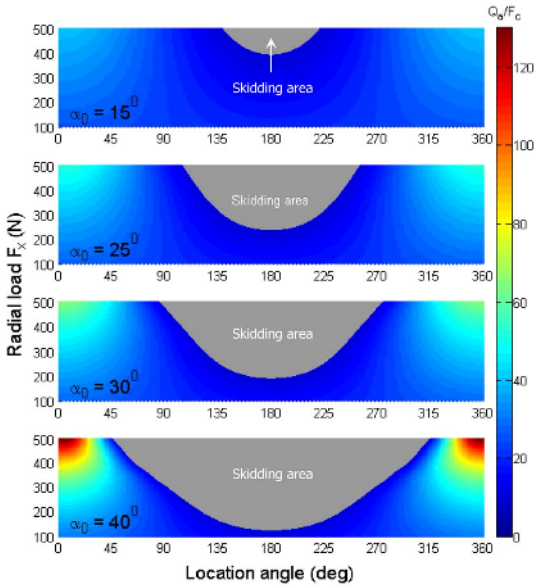

Fig. 15. Effect of unloaded contact angle on the skidding of ACBB under radial loading (n = 5000 rpm, F_z = 400 N).

predicting the skidding of ACBBs, by adopting Hirano's criterion with a quasi-static ACBB model. Based on this method, we have investigated the skidding of a sample ACBB, considering the influence of the rotational speed, combined loads, and angular misalignment. The effects of the unloaded contact angle and preloading method on the skidding were also analyzed. Through simulation and analysis, the following conclusions were drawn:

(1) At a certain rotational speed, there exists a minimum axial preload, under which the skidding phenomenon in ACBBs does not occur. With increasing rotational speed, the required axial preload increases nonlinearly. Increasing ball centrifugal force and decreasing contact force between the ball and inner race are two major factors leading to the increased skidding in the bearing with increasing the rotational speed.

(2) In the case of an aligned bearing, an increased radial load enlarges the skidding area, which occurs around the circumferential angle 180°.

(3) Angular misalignment can introduce skidding areas in an ACBB preloaded by the constant-force method. The skidding does not increase owing to angular misalignment when using the constant-displacement preload method, because an additional axial load is induced.

(4) When a radial load is applied to a misaligned ACBB, there exist two more-probable skidding regions around the circumferential angles of 90° and 270°. Increasing the radial load will increase the skidding area, which is caused by the reduction in the ball–inner race contact force at the corresponding location angles.

(5) The unloaded contact angle has little effect on the skidding of an ACBB subjected to axial loading. However, the unloaded contact angle significantly increases the skidding areas under radial loading.

Acknowledgements

This research was financially supported by Kumoh National Institute of Technology, Korea.

References

[1] T. A. Harris, *Rolling Bearing Analysis*, 4th Ed., John Wiley and Sons (2001).

[2] P. K. Gupta, Current status of and future innovations in rolling bearing modeling, *Tribology Transactions*, 54 (3) (2011) 394-403.

[3] S. W. Hong and V. C. Tong, Rolling-element bearing modeling: A review, *International Journal of Precision Eng. and Manufacturing*, 17 (12) (2016) 1729-1749.

[4] V. C. Tong and S. W. Hong, Modeling and analysis of double-row cylindrical roller bearings, *Journal of Mechanical Science and Technology*, 31 (7) (2017) 3379-3388.

[5] F. Hirano and H. Tanoue, Motion of a ball in a ball bearing, *Wear*, 4 (3) (1961) 177-197.

[6] F. Hirano, Motion of a ball in angular contact ball bearing, *ASLE Transactions*, 8 (4) (1965) 425-434.

[7] R. Boness, Minimum load requirements for the prevention of skidding in high speed thrust loaded ball bearings, *Journal of Lubrication Technology*, 103 (1) (1981) 35-39.

[8] N. T. Liao and J. F. Lin, Ball bearing skidding under radial and axial loads, *Mechanism and Machine Theory*, 37 (1) (2002) 91-113.

[9] T. Xu et al., A preload analytical method for ball bearings utilising bearing skidding criterion, *Tribology International*, 67 (2013) 44-50.

[10] T. A. Harris, An analytical method to predict skidding in high speed roller bearings, *ASLE Transactions*, 9 (3) (1966) 229-241.

[11] T. A. Harris, An analytical method to predict skidding in thrust-loaded, angular-contact ball bearings, *Journal of Lubrication Technology*, 93 (1) (1971) 7-23.

[12] R. J. Boness and C. R. Gentle, Ball motion in thrust loaded ball bearings, *Wear*, 35 (1) (1975) 131-148.

[13] C. R. Gentle and R. J. Boness, Prediction of ball motion in high-speed thrust-loaded ball bearings, *Journal of Lubrication Technology*, 98 (3) (1976) 463-469.

[14] J. Li et al., An improved quasi-dynamic analytical method to predict skidding in the roller bearing under the conditions of extremely light loads and whirling, Strojniški vestnik - *Journal of Mechanical Engineering*, 62 (2) (2016) 86-94.

[15] S. Jain and H. Hunt, A dynamic model to predict the occurrence of skidding in wind-turbine bearings, *Journal of Physics: Conference Series*, 305 (1) (2011) 012027-1-012027-10.

[16] W. Tu, Y. Shao and C. K. Mechefske, An analytical model to investigate skidding in rolling element bearings during acceleration, *Journal of Mechanical Science and Technology*, 26 (8) (2012) 2451-2458.

[17] Y. Wang et al., Investigation of skidding in angular contact ball bearings under high speed, *Tribology International*, 92

(2015) 404-417.
[18] Q. Han and F. Chu, Nonlinear dynamic model for skidding behavior of angular contact ball bearings, *Journal of Sound and Vibration*, 354 (2015) 219-235.
[19] Q. Han, X. Li and F. Chu, Skidding behavior of cylindrical roller bearings under time-variable load conditions, *International Journal of Mechanical Science*, 135 (2018) 203-214.
[20] B. Fang et al., Determination of optimum preload considering the skidding and thermal characteristic of high-speed angular contact ball bearing, *Journal of Mechanical Design*, 140 (5) (2018) 053301.
[21] J. M. de Mul, J. M. Vree and D. Maas, Equilibrium and associated load distribution in ball and roller bearings loaded in five degrees of freedom while neglecting friction-Part I: General theory and application to ball bearings, *Journal of Tribology*, 111 (1) (1989) 142-148.
[22] V. C. Tong and S. W. Hong, Study on the running torque of angular contact ball bearings subjected to angular misalignment, *Journal of Engineering Tribology*, 232 (7) (2018) 890-909.
[23] V. C. Tong and S. W. Hong, The effect of angular misalignment on the running torques of tapered roller bearings, *Tribology International*, 95 (2016) 76-85.
[24] V. C. Tong and S. W. Hong, Improved formulation for running torque in angular contact ball bearings, *International Journal of Precision Engineering and Manufacturing*, 19 (1) (2018) 47-56.
[25] NSK Ltd., *Rolling Bearing Catalogue, CAT. No. E1102m*, Japan (2013).
[26] SKF Group, *SKF General Catalogue, 6000/I EN*, Sweden (2008).
[27] E. V. Zaretsky, W. J. Anderson and R. J. Parker, The effect of contact angle on rolling-contact fatigue and bearing load capacity, *ASLE Transactions*, 5 (1) (1962) 210-219.

Appendix

The displacements of the inner ring cross-section and contact load are defined, respectively, by (see Fig. A.1(a))

$$\{u\}^{\mathrm{T}} = \{u_r, u_x, \theta\} \tag{A.1}$$

$$\{Q\}^{\mathrm{T}} = \{Q_r, Q_x, T\} \tag{A.2}$$

where $\{u\}$ depends on the global displacement by

$$\{u\} = [R\phi]\{\delta\} \tag{A.3}$$

where the transformation matrix is given by

$$[R\phi] = \begin{bmatrix} \cos\phi & \sin\phi & 0 & -z_P\sin\phi & z_P\cos\phi \\ 0 & 0 & 1 & r_P\sin\phi & -r_P\cos\phi \\ 0 & 0 & 0 & -\sin\phi & \cos\phi \end{bmatrix}. \tag{A.4}$$

The ball center displacement is indicated by

$$\{v\}^{\mathrm{T}} = \{v_r, v_x\}. \tag{A.5}$$

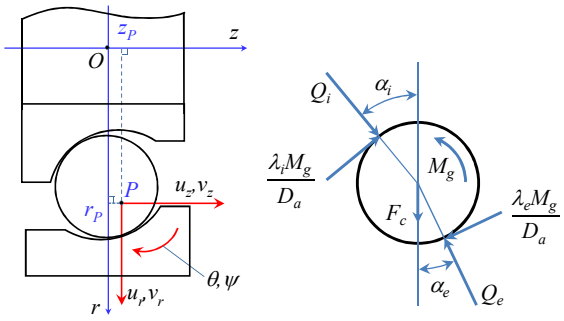

Fig. A.1. Equilibrium of a ball: (a) Local coordinate system defined at a particular ball; (b) free-body diagram of a ball.

The ball loading including the ball–race contact forces, centrifugal force, and gyroscopic moment is shown in Fig. A.1(b). The equilibrium equations of a ball are given as follows:

$$\begin{Bmatrix} Q_i\cos\alpha_i - Q_e\cos\alpha_e + F_c - \dfrac{\lambda_i M_g}{D_a}\sin\alpha_i + \dfrac{\lambda_e M_g}{D_a}\sin\alpha_e \\ Q_i\sin\alpha_i - Q_e\sin\alpha_e + \dfrac{\lambda_i M_g}{D_a}\cos\alpha_i - \dfrac{\lambda_e M_g}{D_a}\cos\alpha_e \end{Bmatrix} = \begin{Bmatrix} 0 \\ 0 \end{Bmatrix} \tag{A.6}$$

where λ_i and λ_e indicate the distribution parameters for the gyroscopic moment. The effects of gyroscopic moment on each raceway are assumed equal, i.e., $\lambda_i = \lambda_e = 1$. The centrifugal force and gyroscopic moment of a ball are calculated by

$$F_c = \frac{1}{2} m d_m \omega_m^2 \tag{A.7}$$

$$M_g = J\omega_m\omega_R\sin\beta \tag{A.8}$$

where the pitch angle β is defined as the angle between the bearing axis and rolling axis of the ball, which can be calculated using a simple geometric relationship as

$$\beta = \frac{\alpha_i + \alpha_e}{2}. \tag{A.9}$$

The ball orbital speed and spinning speed can be calculated by

$$\omega_m = \omega\left(1 + \frac{(1+\gamma\cos\alpha_e)(\cos\alpha_i + \tan\beta\sin\alpha_i)}{(1-\gamma\cos\alpha_i)(\cos\alpha_e + \tan\beta\sin\alpha_e)}\right)^{-1} \tag{A.10}$$

$$\omega_R = \frac{-\omega}{\gamma\cos\beta}\left(\frac{\cos\alpha_e + \tan\beta\sin\alpha_e}{1+\gamma\cos\alpha_e} + \frac{\cos\alpha_i + \tan\beta\sin\alpha_i}{1-\gamma\cos\alpha_i}\right)^{-1} \tag{A.11}$$

where

$$\gamma = \frac{D_a}{d_m}. \tag{A.12}$$

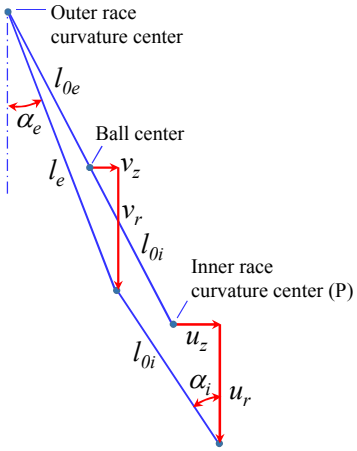

Fig. A.2. Position of ball center, inner and outer race curvature center before and after loading.

The ball contact forces are calculated by the Hertzian theory

$$Q_i = K_i \delta_i^{3/2} \tag{A.13}$$

$$Q_e = K_e \delta_e^{3/2} \tag{A.14}$$

where K_i and K_e are the contact constants depending on the material and geometry at the contact [1]. The contact deformation can be calculated from the geometric relationships shown in Fig. A.2 as follows:

$$\delta_i = l_i - l_{0i} \tag{A.15}$$

$$\delta_e = l_e - l_{0e} \tag{A.16}$$

$$\alpha_i = \tan^{-1} \frac{l_{0i} \sin\alpha_0 - v_z + u_z}{l_{0i} \cos\alpha_0 - v_x + u_x} \tag{A.17}$$

$$\alpha_e = \tan^{-1} \frac{l_{0e} \sin\alpha_0 + v_z}{l_{0e} \cos\alpha_0 + v_x} \tag{A.18}$$

$$l_i = \frac{l_{0i} \sin\alpha_0 - v_z + u_z}{\sin\alpha_i} \tag{A.19}$$

$$l_e = \frac{l_{0e} \sin\alpha_0 + v_z}{\sin\alpha_e} \tag{A.20}$$

where the subscripts e and i denote the outer and inner race, respectively, and the subscript 0 indicates the initial value. The contact load of the inner race is given by

$$\{Q\} = \begin{Bmatrix} -Q_i \cos\alpha_i + M_g / D \sin\alpha_i \\ -Q_i \sin\alpha_i - M_g / D \cos\alpha_i \\ 0.5 M_g / D \end{Bmatrix}. \tag{A.21}$$

A summation of the external load and all contact loads acting on the inner ring gives the global equilibrium of bearing as

$$\{F\} + \sum_{j=1}^{n} [R\phi]^T \{Q\}_j = \{0\}. \tag{A.22}$$

Laily Oktaviana received her B.S. degree in Engineering Physics from Sepuluh Nopember Institute of Technology, Indonesia in 2017. She is currently a graduate student in Mechanical System Engineering at Kumoh National Institute of Technology, Korea.

Van-Canh Tong received his M.S. degree in Mechanical Engineering from Hanoi University of Science and Technology, Vietnam in 2011. He earned his Ph.D. degree in Mechatronics from Kumoh National Institute of Technology, Korea in 2017. He is currently a Postdoctoral researcher at Korea Institute of Machinery & Materials.

Seong-Wook Hong received his M.S. and Ph.D. degrees in Mechanical Engineering from KAIST, Korea, in 1985 and 1989, respectively. Currently, he is a Professor in the Department of Mechanical System Engineering of Kumoh National Institute of Technology. His current research interests include spindle and bearings modeling and analysis, command shaping for positioning systems, vibration control, and structural vibration analysis for mechanical systems.